Protease degradable electrospun fibrous hydrogels

Ryan J. Wade[1,2], **Ethan J. Bassin**[2], **Christopher B. Rodell**[2], and **Jason A. Burdick**[2,*]

[1]Department of Materials Science and Engineering, University of Pennsylvania, Philadelphia, Pennsylvania 19104

[2]Department of Bioengineering, University of Pennsylvania, Philadelphia, Pennsylvania 19104

Abstract

Electrospun nanofibers are promising in biomedical applications to replicate features of the natural extracellular matrix (ECM). However, nearly all electrospun scaffolds are either non-degradable or degrade hydrolytically, whereas natural ECM degrades proteolytically, often through matrix metalloproteinases (MMPs). Here, we synthesize reactive macromers that contain protease-cleavable and fluorescent peptides and are able to form both isotropic hydrogels and electrospun fibrous hydrogels through a photoinitiated polymerization. These biomimetic scaffolds are susceptible to protease-mediated cleavage *in vitro* in a protease dose dependent manner and *in vivo* in a subcutaneous mouse model using transdermal fluorescent imaging to monitor degradation. Importantly, materials containing an alternate and non-protease-cleavable peptide sequence are stable in both *in vitro* and *in vivo* settings. To illustrate the specificity in degradation, scaffolds with mixed fiber populations support selective fiber degradation based on individual fiber degradability. Overall, this represents a novel biomimetic approach to generate protease-sensitive fibrous scaffolds for biomedical applications.

Keywords

Fibrous; Scaffolds; Electrospinning; Degradable; Matrix Metalloproteinase

An increased understanding of the contributions of extracellular matrix (ECM) structural features (e.g., fiber size and orientation) in guiding tissue function has motivated researchers to create biomimetic scaffolds with increased structural complexity[1]. In particular, three methods – self-assembly[2,3], phase separation[4,5], and electrospinning[6,7] – have emerged as techniques to generate fibrous scaffolds with electrospinning becoming the most ubiquitous method due to its ease of setup, scalability, and feasibility with a diverse array of polymers. A wide variety of natural and synthetic polymers have been electrospun and demonstrated

*burdick2@seas.upenn.edu.

utility in various biomedical applications including vascular grafts[8], drug delivery[9], contraception and sexually transmitted disease prevention[10], and cardiac[11,12], skeletal[13,14], dermal[15], and craniofacial[16] tissue formation. Together, these and other studies have indicated that scaffold structural features can influence cell morphology[14], alignment[17], migration[18], differentiation[19], and tissue organization[13].

Despite the success of these materials in replicating the anisotropic, fibrous structure of natural ECM, the majority of electrospun materials are synthetic (non-bioactive) and hydrophobic and/or semi-crystalline (i.e. polycaprolactone, poly(lactic acid), poly(lactic-co-glycolic acid)) such that fibers are rigid with limited water absorption, in stark contrast to the bioactive, flexible, hydrated state of natural ECM. Moreover, these electrospun scaffolds are either non-degradable or degrade hydrolytically, through passive release determined by material crystallinity, hydrophobicity, and stability of the polymer backbone to hydrolysis. Meanwhile, natural ECM components are bioactive and degrade proteolytically, through dynamic interactions with matrix metalloproteinases (MMPs) that are actively regulated in natural ECM remodeling[20,21].

As an alternative to synthetic polymers, components of natural ECM such as proteins have also been electrospun[22]. Since Matthews *et al.* first electrospun Type I and Type III collagen in 2002[23], other natural proteins such as other types of collagen[24], gelatin[25], fibrinogen[26], and elastin[24] have been electrospun. These electrospun scaffolds exhibit some level of bioactivity, mimic features of the flexible, hydrated state of natural soft tissue microenvironments, and may be enzymatically degradable due to their primary amino acid sequence[22]. However, these hydrophilic scaffolds require crosslinking to stabilize the structural features of the scaffold upon introduction to aqueous environments. This crosslinking with gluteraldehyde[27] or other agents[22] may present toxicity issues, and modifications of the natural polymers (e.g. crosslinking of amines) may limit their bioactivity. Not surprisingly, electrospinning may damage secondary and higher order protein structure such that only ~42% of the characteristic spacing between each polyproline-II helix of natural collagen is retained after electrospinning[28]. Structural differences between natural and electrospun proteins are further compounded by batch-to-batch variations of proteins purified from animal sources[29]. From an engineering view, perhaps the most striking limitation of electrospun natural proteins is the limited ability to alter many of their properties, including enzymatic degradation. The primary amino acid sequence and conformation of the protein dictates the rate of enzymatic cleavage, neither of which may be effectively controlled through electrospinning.

Isotropic hydrogels have been synthetically crosslinked with protease degradable peptides to combine the benefits of enzymatic degradability with material tunability[30–35]. Studies have illustrated that this protease-mediated degradation is an important regulator in bone formation[30], angiogenesis[31], and tissue function after myocardial infarction[35]. However, the chemistry and crosslinking used in these studies relies on spontaneous gelation after mixing reagents and is not compatible with electrospinning; thus, proteases-sensitive degradation has not yet been translated to synthetic fibrous hydrogels.

Here, we report an approach to create protease degradable electrospun hydrogels through chemical modification of hyaluronic acid (HA – a linear polysaccharide composed of alternating d-glucuronic acid and N-acetyl-d-glucosamine), combining the bioactivity of a natural polymer with the importance of engineered enzymatic sensitivity. We demonstrate that isotropic hydrogels and electrospun hydrogels crosslink through photopolymerizable peptides and swell upon hydration. *In vitro* and *in vivo,* scaffold degradation behavior in the presence of exogenously added or natural proteases varies when a protease degradable or non-degradable peptide is incorporated. To our knowledge, this approach represents the first electrospun hydrogel that degrades through engineered protease sensitivity.

Results

Design of protease sensitive photocrosslinkable HA

HA was chosen as the primary macromer component because it is a bioactive molecule of natural ECM and is microbially sourced to limit purification concerns associated with ECM proteins sourced from animals. Furthermore, HA has a repeat structure with several functional groups (e.g. hydroxyls, carboxyls) amenable to chemical modification and may contain several hundred repeat units to enable varying degrees of functionalization[36]. Previous studies have also successfully electrospun methacrylate functionalized HA into scaffolds consisting of stable, water-swollen fibers that mimic the microenvironments of many soft tissues[37]. Conceptually, we hypothesized that by incorporating a protease degradable or non-degradable sequence between the methacrylate group and HA backbone, we could generate a starting material that would crosslink through methacrylates and degrade through the specificity of the designed peptide sequence.

With this goal in mind, we took a modular approach to macromer synthesis consisting of three steps – synthetic modification of HA with maleimides, synthesis of methacrylated peptides and fluorophore peptides with terminal thiols as nucleophiles for Michael addition, and modular attachment of peptides via thiol-maleimide Michael addition. In the first step, maleimide HA (MaHA) was synthesized by reacting maleimide salt with tetrabutylammonium-HA (soluble in organics) via a BOP coupling agent ((Benzotriazol-1-yloxy)tris(dimethylamino)phosphonium hexafluorophosphate) to form an amide linkage between the carboxyl group of HA and the amine group of the maleimide salt (Fig. 1a., Supplementary Fig. 1). Maleimides are known to undergo near quantitative, rapid (seconds-minutes) click reactions with thiols that allows for efficient conjugation of photopolymerizable peptides[38]. Compared to previously reported esterification modifications of HA[34], the amide linkage between the maleimide group and HA was chosen to limit hydrolysis of the linkage after peptide conjugation.

Second, thiolated peptides (containing a cysteine amino acid) were synthesized with terminal methacrylate groups or fluorophores by adding methacrylic acid or carboxylated fluorophores (Rhodamine B, FITC, Cyanine7.5), respectively, as the terminal reactant in solid-phase peptide synthesis (Fig. 1b and 1c). Thiolated fluorophores (GCKK-Rho, GCKK-FITC, GCKKG-Cyanine7.5) were synthesized to directly label HA with fluorescent dyes to accurately quantify HA erosion from scaffolds *in vitro* (GCKK-Rho, GCKK-FITC) and *in vivo* (GCKKG-Cyanine7.5); therefore, their excitation and emission spectra were analyzed

to aid in subsequent fluorometric spectroscopy (Fig. 1b). The protease degradable peptide (Fig. 1c) was based on previous studies that indicated enhanced susceptibility to MMP-1 and MMP-2 mediated cleavage within the central 8 amino acid sequence[31]. The non-degradable peptide (Fig. 1c) is a novel sequence that was designed to be resistant to degradation by numerous enzymes (i.e. MMPs, pepsin, trypsin) and contain the same number of amino acids as the protease degradable peptide to aid in comparisons between the two sequences. To evaluate the proteolytic sensitivity, peptides were placed at varying concentrations into recombinant human MMP-2 (rhMMP-2) or Type II collagenase (broad range of proteases) to determine the kinetic parameters for protease-mediated cleavage using a modified fluorescamine assay[30,31,39]. The protease degradable peptide followed Michaelis-Menten kinetics (Table 1, Supplementary Fig. 2) in rhMMP-2 and collagenase and had kinetic parameters similar to those previously reported in rhMMP-2[31]; however, the non-degradable peptide kinetic parameters were not measurable as cleavage was not detectable for the duration of the assay (9 hours).

In the final step, peptides were conjugated to MaHA by first mixing thiolated fluorophores with MaHA to consume a small portion of maleimides. Next, excess methacrylated peptide was added to consume all remaining maleimide groups, and the product was dialyzed and lyophilized to yield the macromer, Methacrylated Peptide HA (MePHA) (Fig. 1a). For consistency, GCKK-Rho was conjugated to all non-degradable MePHA (crosslinks through non-degradable peptide) and GCKK-FITC to all protease degradable MePHA (crosslinks through protease degradable peptide) for all subsequent *in vitro* characterization. GCKKG-Cyanine7.5 was conjugated to both protease degradable and non-degradable MePHA used *in vivo*.

Isotropic hydrogel formation and characterization

After MePHA synthesis, isotropic, non-fibrous hydrogels were fabricated to evaluate the sensitivity of the different MePHA formulations (protease degradable and non-degradable) to enzyme-mediated degradation. Furthermore, the formation of isotropic hydrogels allows for comparison to previous reports of non-fibrous, protease degradable hydrogels[30,31,35,40,41]. Isotropic MePHA hydrogels were formed as 4 wt% or 2 wt% cylindrical discs via UV mediated radical crosslinking with Irgacure 2959 (I2959) as a radical photoinitiator in TTC buffer (Tris, Triton X-100, $CaCl_2$). To ensure similar mechanical properties between different MePHA formulations, storage moduli were measured by oscillatory rheology. Protease degradable hydrogels at 2 wt% (250 ± 14 Pa) and 4 wt% (1.18 ± 0.46 kPa) showed no statistical differences between moduli of equivalent hydrogels of non-degradable MePHA at 2 wt% (300 ± 60 Pa) and 4 wt% (1.51 ± 0.08 kPa), indicating similar gelation between different MePHA formulations (Supplementary Fig. 3). For degradation studies, MePHA hydrogels were incubated in TTC buffer for 48 hours at 37°C and retained their cylindrical shape (Fig. 2a, 2b). Hydrogels were subsequently placed into varying concentrations of Type II collagenase (1 to 500 U ml^{-1}), rhMMP-2 (5 nM), or TTC buffer and monitored for HA release. Collagenase contains a broad range of MMPs and facilitates general comparison with previous reports of protease degradable hydrogels eroded with collagenase[33,41]. Alternatively, rhMMP-2 was chosen to assess degradation in

the presence of a specific MMP at a concentration that is indicative of previously reported physiologic concentrations (1–20 nM)[42–45].

Isotropic protease degradable MePHA hydrogels eroded (i.e. 100% of HA released) within a day to up to 6 days in response to rhMMP-2 and varying collagenase concentration (Fig. 2c, 2e, Supplementary Fig. 4). These rhMMP-2 and collagenase dependent degradation rates agree with previously reported isotropic HA hydrogels crosslinked via addition of MMP-sensitive di-thiol peptides[41]. When incubated in buffer, isotropic protease degradable MePHA hydrogels retained greater than 80% of their original HA content after 18 days incubation in buffer, demonstrating the stability of the hydrogel to non-enzymatic degradation. Conversely, all non-degradable MePHA hydrogels retained greater than 80% of their original HA content, irrespective of the presence of rhMMP-2, or concentration of collagenase within the tested range (Fig. 2d, 2f, Supplementary Fig. 4). Together with the kinetic parameters of the individual methacrylated peptides, this result further indicates that erosion of these hydrogels occurs through protease-mediated cleavage of the peptide crosslinker. Notably, previous erosion studies of hydrogels crosslinked with amino acid sequences insensitive to protease-mediated cleavage were completed in low concentrations of specific recombinant MMPs[30,31], whereas the study reported here also demonstrates resistance to enzyme-mediated degradation in high concentrations of a broad range of proteases.

Electrospun fibrous hydrogel formation and characterization

To generate electrospun fibrous hydrogels, solutions of MePHA (1 wt%) and PEO (4.5 wt %) were mixed with I2959 in TTC buffer and electrospun as thin films (10–30 μm) on methacrylated coverslips (for optical microscopy) or as standalone mats (~1 mm dry thickness, for *in vitro* degradation studies) (Fig. 3a). Electrospun scaffolds were exposed to UV light to initiate radical crosslinking (Fig. 3a) and then further crosslinked with additional light exposure upon hydration to stabilize fibers in their swollen state. Aqueous solutions of HA have a relatively high surface tension at low HA concentrations which limits molecular entanglement and the ability to form smooth electrospun nanofibers[46]; therefore, PEO was included as a bioinert, hydrophilic polymer to increase molecular chain entanglement at lower HA concentrations to improve fiber morphology.

Electrospun scaffolds were characterized by unconfined compression testing and by SEM (dry scaffolds) and confocal microscopy (dry and hydrated scaffolds) to investigate fiber morphology, diameter, and swelling behavior. Similar bulk compressive moduli were observed in protease degradable (2.8 ± 1.0 kPa) and non-degradable (3.4 ± 0.7 kPa) MePHA scaffolds. Meanwhile, SEM indicated smooth fiber morphology throughout scaffolds and submicron diameters for both protease degradable (320 ± 100 nm) and non-degradable (270 ± 60 nm) MePHA scaffolds (Fig. 3b, 3f, Supplementary Fig. 5). When analyzing fiber morphology and diameter in the dehydrated state, artifacts may be introduced in SEM during drying (e.g. alcohol dehydration, flash freezing/lyophilization, critical point drying). Consequently, fiber diameters of fluorescently labeled dry and hydrated scaffolds were also measured *in situ* using confocal microscopy to determine the degree of fiber swelling (Fig. 3c–e, 3g–i). Protease degradable MePHA fiber diameters increased from 590 ± 100 nm

before hydration to 1.27 ± 0.31 µm at equilibrium swelling, and non-degradable MePHA fiber diameters increased similarly from 640 ± 100 nm before hydration to 1.17 ± 0.29 µm at equilibrium swelling. Scaffold porosity was also quantified by confocal microscopy and indicated high porosity in both protease degradable (82 ± 4 %) and non-degradable (79 ± 4 %) MePHA scaffolds. No significant differences existed between bulk compressive modulus, fiber diameters, or porosity of protease degradable and non-degradable MePHA, demonstrating that both electrospun hydrogels display similar mechanical properties and swelling behavior.

To investigate the enzyme-mediated degradation of electrospun protease degradable and non-degradable MePHA, fibrous scaffolds were placed into TTC buffer, rhMMP-2 (10 nM), or Type II collagenase ($5 - 500$ U ml^{-1}) and HA release was monitored (Fig. 4a, 4e, Supplementary Fig. 6). Protease degradable MePHA scaffolds showed a collagenase concentration dependent burst release of degradation products within the first 48 hours, with greater than 80% of HA released from the networks across all collagenase concentrations at 2 weeks; however, in the absence of collagenase these scaffolds retained over 75% of MePHA content after three weeks (Fig. 4a). In comparison, non-degradable MePHA scaffolds all retained greater than 75% of MePHA content after three weeks, regardless of collagenase concentration (Fig. 4e), showing similar degradation profiles to those observed in isotropic, non-fibrous hydrogels (Fig. 2d). Similar trends were also observed in rhMMP-2 as protease degradable scaffolds released nearly 30% of HA after 8 days compared to 6% release of HA in non-degradable scaffolds (Supplementary Fig. 6). Interestingly, all protease degradable scaffolds degraded more rapidly at early time points but slowed in degradation at later time points. HA release from protease degradable MePHA at later time points in collagenase and rhMMP-2 was greater than the passive release observed in TTC buffer, suggesting that protease mediated degradation was still occurring within the scaffolds for the duration of the study, albeit at slower rates.

To ensure that the chemical structure of the protease degradable peptide was not damaged by UV exposure during crosslinking (thus altering the sensitivity of the peptide), methacrylated protease-cleavable peptides were exposed to equivalent UV treatment and analyzed via MALDI-TOF. No changes in molecular weight with UV exposure were observed (Supplementary Fig. 7). To ensure the profiles were not the result of fluorophore cleavage from the HA backbone, degradation was also analyzed via uronic acid assay (Supplementary Fig. 8), confirming the same general profile observed via fluorometric analysis. Previous models of hydrolytic degradation of hydrogels formed through multi-vinyl crosslinks[47] indicate that at early time points, erosion occurs primarily through release of the crosslinking molecule from the network, followed by a plateau of degradation products until kinetic chains are finally released very late upon reverse gelation. The erosion of the protease degradable electrospun MePHA scaffolds reported here follows a similar profile, suggesting that HA release (crosslinking molecule) dominates the initial degradation profile with a corresponding general plateau in degradation rate at later time points until all kinetic chains are released from the network.

To observe fiber degradation *in situ*, thin films of fluorescent protease degradable and non-degradable MePHA were attached to methacrylated glass slides and imaged at different

times within collagenase (500 U ml^{-1}) or TTC buffer (Fig. 4b–d, 4f–h). Similar to the trends observed in free-swelling mats, protease degradable MePHA fibers eroded in collagenase but remained stable in TTC buffer, while all non-degradable MePHA scaffolds remained intact for the duration of the study. To further visualize fiber degradation, dual-phase scaffolds were created by co-electrospinning separate solutions of protease degradable and non-degradable MePHA (Fig. 5a). This process generates fibrous hydrogels with biphasic (protease-mediated and passive) degradation and permits visualization of protease degradable and non-degradable fiber erosion within the same scaffold (Fig. 5b, 5c). Accordingly, we observed enzyme-mediated degradation of the protease degradable fibers, whereas non-degradable fibers retained their structure after 10 days incubation in collagenase (500 U ml^{-1}).

In vivo erosion of electrospun scaffolds was investigated by covalently attaching a near-infrared peptide dye (GCKKG-Cyanine7.5) to MePHA, subcutaneously implanting scaffolds in a murine model, and monitoring the corresponding loss in signal intensity over a 6 week period (Fig. 6). Protease degradable MePHA scaffolds demonstrated faster erosion *in vivo* over the first three weeks (losing nearly 50% of the NIR signal) with considerably slower erosion thereafter. Thus, the *in vivo* erosion follows a similar trend to *in vitro* degradation profiles, with the fastest rates of degradation at earlier times and progressively slower degradation at later times. Relative protease levels may also contribute to the observed *in vivo* erosion profile since MMP activity is known to increase during natural ECM remodeling immediately following tissue injury[42]. It is worth noting that *in vivo* erosion requires degradation and clearance of HA from the tissue, whereas *in vitro* degradation is monitored in an aqueous environment with fewer diffusion barriers to HA release from the network. In comparison to protease degradable MePHA scaffolds, non-degradable MePHA scaffolds eroded at a more linear rate and retained greater HA content throughout the duration of the study, further offering evidence that proteases mediate the observed degradation of protease degradable MePHA scaffolds *in vivo*. It was not possible to identify distinct scaffold margins histologically, as the scaffolds were encompassed within cellular tissue for both protease degradable and non-degradable formulations (Supplementary Fig. 9). Notably, the differences in degradation between protease degradable and non-degradable MePHA *in vitro* were not as pronounced in the subcutaneous *in vivo* model. The observed differences may be due to several factors including super-physiological protease levels, the absence of protease inhibitors, and limited barriers to diffusive release of HA *in vitro*. In comparison, mechanical stimulation, blood flow perfusion, cell release of soluble and insoluble signals, and clearance from the site of implantation will influence *in vivo* degradation.

Discussion

Fibrous hydrogels are gaining widespread attention in biomedical applications due to their ability to mimic many features of the extracellular matrix; however, most fiber systems are either rigid polymers that lack sensitivity to enzymes or are natural polymers with disrupted biological activity during processing or limited sourcing. Current strategies that focus on engineering protease sensitive surface coatings[48] or protease sensitive surface linkers[49] lack the ability for the electrospun network itself to degrade in response to proteases. To address

these limitations, we developed a generalizable chemical scheme to formulate fluorescently labeled HA macromers that can be electrospun and then crosslinked through methacrylated peptides and degrade through the sensitivity of the incorporated amino acid sequence. In particular, this approach permits material crosslinking in the dry state so that electrospun fibrous structures may be stabilized after scaffold formation. In contrast, common chemical schemes that crosslink hydrogels through addition reactions between peptides and a functionalized polymer (i.e. 4 arm or 8 arm-PEG)[31,50] must be performed in a hydrated state; therefore, they do not translate to electrospinning processes. Two photopolymerizable, protease degradable macromers have been synthesized previously, namely acrylate-PEG-(peptide-PEG)$_m$-acrylate[40], and acrylate-peptide-PEG-peptide-acrylate; however, the former contains a high molecular weight between crosslinks (500 kDa) that may limit its ability to form stable fibers, while the latter contains a considerably lower molecular weight between crosslinks (6.4 kDa) that may limit electrospinning and would require very high concentrations of to crosslink. In comparison, our approach has a low average molecular weight between reactive groups (~15 kDa) and a large molecular weight (~140 kDa) to permit stable crosslinking of fibers. Although the scheme reported here used HA, the approach of grafting methacrylated peptides to a polymer via thiol-maleimide Michael addition is amenable to other polysaccharides or hydrophilic synthetic polymers.

The modular approach presented here further allows for conjugating other amino acids of interest to enhance bioactivity through cell adhesive amino acid sequences such as RGD (derived from fibronectin). Another benefit to this system is the ability to electrospin from a non-organic solvent so that growth factors or other soluble signals may be incorporated within fibers for enzyme-mediated release from the network. This release may also be made biphasic by generating a co-electrospun scaffold of protease degradable and non-degradable MePHA (Fig. 5a) where individual fiber degradation is controlled through the degradation of that fiber. Enzymatically mediated dual-phase erosion could be beneficial in controlling release of the network in response to temporal changes in the microenvironment like those observed in the immune response or during wound healing[20]. As a fibrous hydrogel, the system is best suited to soft-tissue applications and may not be suitable for load bearing tissue applications (e.g. musculoskeletal).

Importantly, this work represents the introduction of protease mediated degradation as a mechanism for erosion in electrospun fibrous hydrogels. Previous reports have demonstrated protease mediated degradation in fibrous scaffolds of self-assembling peptide-amphiphiles (PAs) designed to contain an MMP cleavable central domain[51] and in β-sheet forming multidomain peptides (MDPs) with a central three amino acid MMP cleavable motif[52]. These reports have shown that MMP cleavable PAs lose 70% of their mass at 2 weeks in 2 mg ml^{-1} collagenase (Type IV)[51], and that β-sheet forming MDPs lose 95% of their mass at 2 weeks in 3 mg ml^{-1} collagenase (Type IV)[52]. While our studies were conducted in a different type collagenase (Type II-higher tryptic levels), the electrospun scaffolds reported here lose 75% mass at 2 weeks in significantly lower concentrations of collagenase, 0.015 mg ml^{-1} (5U ml^{-1} – Type II). Self-assembling peptides and PAs are beneficial for their ability to generate nanoscale diameters (~6–8 nm) and their ability to form *in situ*, making them an attractive platform as injectable fibrous materials[51,52]; however, mechanical

robustness and complex design, synthesis, and scalability may limit their widespread use. Conversely, electrospun scaffolds have significantly larger fiber diameters and are not directly injectable; yet, the technique is easy to setup, scalable, and applicable to many polymers. Therefore, incorporating protease mediated degradation into electrospun scaffolds with a generalizable approach may be translatable to a number of materials and applications.

Despite the widespread use of electrospun scaffolds in biomedical applications and the importance of protease-mediated cleavage in biological processes, engineered protease degradation had yet to be explored in electrospun hydrogels. This report makes use of a modular approach to generate electrospinnable macromers that degrade through peptide crosslinks and demonstrates their *in vitro* degradation and *in vivo* erosion profiles. These results present a novel degradation mechanism for engineered electrospun hydrogels, an approach that may benefit *in vitro* and *in vivo* investigations by synthetic inclusion of biochemically relevant degradation within biophysically relevant scaffolds.

Methods

Solid-phase peptide synthesis

All materials are from Sigma-Aldrich unless noted otherwise. Protease degradable peptide (GCNS-*GGRM* ↯ *SMPV*-SNGG-Methacrylate), non-degradable peptide (GCEE-NGGSGGGSN-GGGH-Methacrylate), and thiolated peptide fluorophores (GCKK-FITC, GCKK-Rhodamine, GCKKG-Cyanine7.5) were each synthesized with a thiol to facilitate Michael addition coupling to MaHA. The protease degradable sequence is listed in italics where protease-mediated cleavage is known to occur at the indicated arrow, between the central serine and methionine amino acids. Briefly, peptides were synthesized on Glycinol 2-Chlorotrityl resin (protease degradable, non-degradable, GCKKG-Cyanine7.5) (Novabiochem) or 1,6-Diaminohexane trityl resin (GCKK-FITC, GCKK-Rhodamine) (Novabiochem) using a PS3 automated solid phase peptide synthesizer (Protein Technologies, Inc.) via standard FMOC chemistry. The resin was deprotected with 20% (v/v) piperidine in N,N-dimethylformamide (DMF), and FMOC protected amino acids (Novabiochem) were then activated with HBTU (Novabiochem) and 0.4 M methylmorpholine in DMF before being added to the reaction vessel in 4 times excess to resin functional groups. To add non-amino acid terminal functional groups to the peptides, the corresponding carboxylic acid form of the functional group (methacrylic acid, 5(6)-carboxyflourescein, Rhodamine B, or Cyanine7.5 carboxylic acid (Lumiprobe)) was added in the last step of synthesis. Peptides were cleaved in a 10 mL solution of 95% trifluoroacetic acid, 2.5% triisopropylsilane, and 2.5% DI H_2O, precipitated twice in cold diethyl ether (−80 °C), and allowed to dry overnight.

Peptides were dissolved in DI H_2O, flash frozen in liquid nitrogen, lyophilized, and stored under nitrogen at −20°C until use or analyzed for purity by matrix-assisted laser desorption ionization – time of flight mass spectroscopy (MALDI-TOF) to confirm synthesis (Supplementary Fig. 10, 11). Protease degradable and non-degradable peptides were further analyzed via ^{1}H NMR (Bruker DMX 360 MHz) and the degree of methacrylation per peptide was determined (~100%) by calibrating to known amino acid peaks for valine (protease degradable sequence) or histidine (non-degradable sequence) (Supplementary Fig.

12). Thiolated fluorophore excitation and emission spectra were measured using a Tecan Spectrometer (Fig. 1b).

Degradation kinetics

Kinetic parameters for protease degradable peptides and non-degradable peptides were measured using a modified fluorometric assay as previously published[30,39]. Briefly, peptides (50–500 μM) were incubated with 1 U ml^{-1} Type II Collagenase (Worthington Biochemical) or 1 nM rhMMP-2 (R&D Systems) in fluorescence buffer (50 mM tricine, 50 mM NaCl, 10 mM CaCl$_2$, 0.05% Brij-35, pH 7.4) at 37°C. Substrate cleavage was monitored by reacting 20 μL fluorescamine (50 mM in acetone) with 75 mL of substrate/enzyme solution and detecting fluorescence (excitation: 380 nm, emission: 480 nm) on a Tecan Spectrometer. Initial reaction velocities were determined from plots of fluorescence vs. time. The slope of each plot was divided by the fluorescence corresponding to full hydrolysis, and multiplied by the substrate concentration to give velocity in micromoles per minute. Lineweaver-Burk plots (1/V vs. 1/[S]) were linear for protease degradable peptides, indicating Michaelis-Menten kinetic behavior (Supplementary Fig. 2). Kinetic parameters were determined by directly curve fitting plots of velocity vs. substrate concentration to the Michaelis-Menten equation (to limit errors induced by Lineweaver-Burk double-reciprocal plots). Fluorescence did not increase over time for non-degradable peptides such that their kinetic parameters could not be determined.

MePHA synthesis

MePHA polymers were synthesized in a modular three-step process. First, MaHA was synthesized as previously described[41]. Briefly, Na-HA (90 kDa, Lifecore) was dissolved in DI H$_2$O and a Dowex® 50Wx8 ion-exchange resin and mixed at 600 RPM for 5 hours. The resin was filtered from the reaction vessel and the solution was titrated to pH 7.02–7.05 with tetrabutylammonium hydroxide, frozen, and lyophilized to yield HATBA. Next, HATBA was dissolved as a 2 wt% solution in anhydrous dimethyl sulfoxide (DMSO) (Fisher) and reacted with equivalent molar amounts of N-(2-aminoethyl)maleimide trifluoroacetate salt and BOP ((Benzotriazol-1-yloxy)tris(dimethylamino)phosphonium hexafluorophosphate) under N$_2$ for four hours before dialyzing (8,000 MWCO, Spectra/Por®) against cold DI H$_2$O for two weeks. MaHA solutions were frozen, lyophilized, and analyzed via NMR to determine the degree of HA repeat functionalization with maleimide groups (Supplementary Fig. 13). Although different degrees of maleimide functionalization were achieved (5%–35%) all studies reported here were conducted with 10–15% functionalized MaHA (i.e. 10–15% of HA repeats contain a maleimide linkage) for consistency between all materials. Second, thiolated peptides were synthesized as described above. Third, MaHA was dissolved as a 1 wt% solution in DI H$_2$O and thiolated peptide fluorophore was stoichiometrically added such that thioether bonds would form in less than 6 maleimide repeats per HA polymer chain. 90 kDa HA contains greater than 230 repeat units on average such that 15% modified MaHA contains 35 maleimide repeats, of which less than 6 are consumed by thiolated fluorophore. After 30 minutes of mixing, methacrylated peptide (protease degradable or non-degradable) was added in 1.4 times excess to maleimide groups and allowed to react for 4 hours at room temperature to consume all remaining maleimide groups. The solution was titrated to neutral pH using 5 N sodium hydroxide, dialyzed (8,000

MWCO, Spectra/Por®) against cold DI H_2O for 72 hours, frozen, lyophilized, and stored at $-20°C$. Final product conjugation was confirmed via ^1H NMR by the loss of maleimide peak and introduction of methacrylate peaks from the conjugated peptide (Supplementary Fig. 14).

Scaffold fabrication

All degradation studies (*in vitro* and *in vivo*) were replicated (n=3 or 4 as stated throughout) to determine statistical significance. Prior to any hydration step, all formulations of MePHA were sterilized under germicidal UV exposure for 45 minutes and maintained under sterile conditions thereafter. For rheological studies, solutions of 2 and 4 weight percent MePHA with 0.05% Irgacure 2959 (I2959) in TTC buffer (0.05% Triton X-100, 50 mM Tris-HCl, 1 mM $CaCl_2$, pH 7.4) were exposed to 10 mW cm^{-2} of UV light (Omnicure s1000 – 365 nm filter) for 15 minutes on an AR2000 stress-controlled rheometer (TA instruments - 20 mm diameter cone and plate geometry, 59 min 42 s cone angle, and a 27 µm gap distance) under 0.1% oscillatory strain. To synthesize isotropic MePHA hydrogels for degradation studies, 50 µl solutions of 4 wt% or 2 wt% MePHA with 0.05% I2959 in TTC buffer were contained in a cylindrical mold (tip of a cut 1mL syringe) and exposed to 10 mW cm^{-2} UV light for 15 minutes to induce gelation.

To synthesize electrospun fibrous MePHA hydrogels, solutions of 1 wt% MePHA, 4.5 wt% PEO (900 kDa), and 0.05 wt% I2959 in TTC Buffer were mixed at 110 RPM for 24–48 hours and loaded into syringes. These solutions were then electrospun onto a rotating mandrel (350 RPM to maintain random fiber orientation during collection) in a custom environmentally regulated chamber (humidity 20–35%) with the following collection parameters: applied voltage: 21–26 kV, deflector voltage: 10–12 kV, collector voltage: –3 kV, distance from needle to collector – 18 cm, needle gauge – 18, flow rate: 1.0 ml hr^{-1}. Dual electrospun mats used two separate syringes facing the rotating collection mandrel from opposite sides (Fig. 5a). To image electrospun fibrous MePHA hydrogels, fibers were collected onto aluminum foil and imaged with a FEI Quanta 600 environmental scanning electron microscope, or collected onto methacrylated coverslips[53] and imaged using confocal fluorescent microscopy (Zeiss Axio Observer Inverted microscope) or wide field fluorescent microscopy (Olympus BX51). To crosslink electrospun MePHA hydrogels, dry scaffolds were exposed to 30 minutes of 10 mW cm^{-2} UV light under N_2, swollen with 0.05% I2959 in TTC buffer and re-exposed to 10 mW cm^{-2} UV light for 1 minute (thin films (10–30 µm) for confocal imaging – to limit photobleaching) or 20 mW cm^{-2} UV light for 30 minutes (for degradation studies). To determine fiber diameters, scaffolds were imaged in 8 distinct scaffold areas and fiber diameters were quantified using Image J (>25 fibers per image, 63X magnification – confocal, 9500X magnification – SEM). Similar to the method previously described[54], scaffold porosity was determined by converting confocal images (63X magnification) of thin electrospun films to binary, thresholding the images, and quantifying the void area of the image as a percentage of the total area (ImageJ, >6 images per condition). Unconfined compression testing was performed on swollen electrospun hydrogels using a TA Instruments DMA Q800 at constant strain rate of 10% per minute. Compressive modulus was calculated from the slope of the stress-strain curve between 5 and 15% strain (n=3).

Degradation studies

Isotropic hydrogels (50 μl) were equilibrated at 37°C in 1 ml of TTC for 48 hours in lo-bind tubes and then placed into fresh sterile TTC Buffer, 5nM rhMMP-2, or sterile 1–500 U ml^{-1} Type II Collagenase (stock activity – 335 U mg^{-1}, Worthington Biochemical) in TTC buffer (n=3 per condition). Units of activity are given by Worthington Biochemical COA and defined as "one unit liberates one micromole of L-leucine equivalents from collagen in 5 hours at 37°C, pH 7.5". Fibrous hydrogels electrospun as thin films and thick mats (1 cm^2 area ~ 1 mm thick dry) were equilibrated at 37°C in TTC Buffer for 48 hours in a non-tissue culture treated plate and then refreshed with TTC Buffer, 10nM rhMMP-2 (with 0.1 wt% reagent diluent (R&D systems) to limit rhMMP-2 adsorption to well surfaces), or 5–500 U ml^{-1} Type II Collagenase in TTC Buffer (n=3,4 per condition). Supernatant was collected and samples were refreshed with the corresponding media every two days to maintain enzymatic activity. Scaffolds not fully degraded at the end of studies were degraded in 1 mg ml^{-1} hyaluronidase to determine total HA content. The collected supernatant was analyzed via fluorometric spectroscopy (FITC - excitation: 480 nm emission: 517nm; RHO – excitation: 550 nm emission: 580 nm; Cyanine7.5 – excitation: 788 nm emission: 818 nm) and compared to a standard curve of equivalent fluorescent MePHA. Individual scaffold degradation was formulated into a percentage and then averaged between groups to generate degradation profiles. Uronic acid (HA repeat units) release was quantified by colorimetric absorbance as previously described[55] to confirm degradation profiles observed by fluorescent MePHA release. To visualize degradation, thin film scaffolds were imaged with an Olympus BX51 microscope at different stages of degradation. Acquisition parameters (i.e. light intensity, camera exposure, resolution) were kept the same for all images to enable comparison between groups. Co-electrospun images were overlaid using Image J, again maintaining equivalent acquisition and processing parameters between compared images.

Subcutaneous mouse model

To evaluate *in vivo* degradation of electrospun fibrous hydrogels, 25 mm^2 scaffolds (MMP degradable or non-degradable, ~1 mm thick dry) conjugated with the GCKKG-Cyanine7.5 fluorophore (near-IR) were equilibrated in sterile PBS for 48 hours (37°C) and then subcutaneously implanted into the dorsal region of adolescent BALB/C mice (male). Serial images were taken during a six-week period using a LiCore live imaging system (800 nm), and signal intensity (photons pixel^{-1} second^{-1}) was measured by integrating equivalent areas over the region of interest. Quantified signal was normalized to peak intensity for individual scaffolds and then averaged to obtain degradation profiles for each scaffold (n=4,3 per condition). At the conclusion of the study, the tissue containing fibrous hydrogels was excised, fixed in formalin, embedded in paraffin, sectioned (5 μm slices) through the height of the scaffold region, and stained with hematoxylin and eosin. The study adhered to the NIH Guide for the Care and Use of Laboratory Animals and was approved by the University of Pennsylvania's Institutional Animal Care and Use Committee.

Statistical analysis

All experimental data is reported as the mean of 3 or 4 individual samples. Single factor ANOVAs were performed for data sets with Tukey's HSD post-hoc testing and statistical significance was considered $p<0.05$.

Supplementary Material

Refer to Web version on PubMed Central for supplementary material.

Acknowledgments

References

1. Wade RJ, Burdick JA. Engineering ECM signals into biomaterials. Mater Today. 2012; 15:454–459.

2. Cui H, Webber MJ, Stupp SI. Self-assembly of peptide amphiphiles: From molecules to nanostructures to biomaterials. Pept Sci. 2010; 94:1–18.

3. Wu EC, Zhang S, Hauser CA. Self-Assembling Peptides as Cell-Interactive Scaffolds. Adv Funct Mater. 2012; 22:456–468.

4. Holzwarth JM, Ma PX. Biomimetic nanofibrous scaffolds for bone tissue engineering. Biomaterials. 2011; 32:9622–9629. [PubMed: 21944829]

5. Palchesko, RN., et al. Springer Handbook of Nanomaterials. Springer; 2013. p. 977-1010.

6. Bhardwaj N, Kundu SC. Electrospinning: a fascinating fiber fabrication technique. Biotechnol Adv. 2010; 28:325–347. [PubMed: 20100560]

7. Ji W, et al. Bioactive electrospun scaffolds delivering growth factors and genes for tissue engineering applications. Pharm Res. 2011; 28:1259–1272. [PubMed: 21088985]

8. Rocco KA, Maxfield MW, Best C, Dean EW, Breuer CK. In Vivo Applications of Electrospun Tissue-Engineered Vascular Grafts: A Review. Tissue Eng Pt B-Rev. 2014; 26:628–640.

9. Yoo HS, Kim TG, Park TG. Surface-functionalized electrospun nanofibers for tissue engineering and drug delivery. Adv Drug Del Rev. 2009; 61:1033–1042.

10. Ball C, Krogstad E, Chaowanachan T, Woodrow KA. Drug-eluting fibers for HIV-1 inhibition and contraception. PloS one. 2012; 7:e49792. [PubMed: 23209601]

11. Huang NF, et al. Myotube assembly on nanofibrous and micropatterned polymers. Nano Lett. 2006; 6:537–542. [PubMed: 16522058]

12. Guex AG, et al. Plasma-functionalized electrospun matrix for biograft development and cardiac function stabilization. Acta Biomater. 2014; 10:2996–3006. [PubMed: 24531014]

13. Nerurkar NL, et al. Nanofibrous biologic laminates replicate the form and function of the annulus fibrosus. Nat Mater. 2009; 8:986–992. [PubMed: 19855383]

14. Kim IL, Khetan S, Baker BM, Chen CS, Burdick JA. Fibrous hyaluronic acid hydrogels that direct MSC chondrogenesis through mechanical and adhesive cues. Biomaterials. 2013; 34:5571–5580. [PubMed: 23623322]

15. Kumbar SG, Nukavarapu SP, James R, Nair LS, Laurencin CT. Electrospun poly (lactic acid-co-glycolic acid) scaffolds for skin tissue engineering. Biomaterials. 2008; 29:4100–4107. [PubMed: 18639927]

16. Li G, et al. Electrospun Fibers for Dental and Craniofacial Applications. Curr Stem Cell Res. 2014; 9:187–195.

17. Kim IL, Mauck RL, Burdick JA. Hydrogel design for cartilage tissue engineering: a case study with hyaluronic acid. Biomaterials. 2011; 32:8771–8782. [PubMed: 21903262]

18. Doyle AD, Wang FW, Matsumoto K, Yamada KM. One-dimensional topography underlies three-dimensional fibrillar cell migration. J Cell Biol. 2009; 184:481–490. [PubMed: 19221195]

19. Christopherson GT, Song H, Mao HQ. The influence of fiber diameter of electrospun substrates on neural stem cell differentiation and proliferation. Biomaterials. 2009; 30:556–564. [PubMed: 18977025]

20. Chang C, Werb Z. The many faces of metalloproteases: cell growth, invasion, angiogenesis and metastasis. Trends Biotechnol. 2001; 11:S37–S43.

21. Visse R, Nagase H. Matrix metalloproteinases and tissue inhibitors of metalloproteinases structure, function, and biochemistry. Circ Res. 2003; 92:827–839. [PubMed: 12730128]

22. Sell SA, et al. The use of natural polymers in tissue engineering: a focus on electrospun extracellular matrix analogues. Polymers. 2010; 2:522–553.

23. Matthews JA, Wnek GE, Simpson DG, Bowlin GL. Electrospinning of collagen nanofibers. Biomacromolecules. 2002; 3:232–238. [PubMed: 11888306]

24. Boland ED, et al. Electrospinning collagen and elastin: preliminary vascular tissue engineering. Front Biosci. 2004; 9:1422–1432. [PubMed: 14977557]

25. Huang ZM, Zhang Y, Ramakrishna S, Lim C. Electrospinning and mechanical characterization of gelatin nanofibers. Polymer. 2004; 45:5361–5368.

26. Wnek GE, Carr ME, Simpson DG, Bowlin GL. Electrospinning of nanofiber fibrinogen structures. Nano Lett. 2003; 3:213–216.

27. Zhong S, et al. Formation of collagen-glycosaminoglycan blended nanofibrous scaffolds and their biological properties. Biomacromolecules. 2005; 6:2998–3004. [PubMed: 16283719]

28. Bürck J, et al. Resemblance of electrospun collagen nanofibers to their native structure. Langmuir. 2013; 29:1562–1572. [PubMed: 23256459]

29. Barnes CP, Sell SA, Boland ED, Simpson DG, Bowlin GL. Nanofiber technology: designing the next generation of tissue engineering scaffolds. Adv Drug Del Rev. 2007; 59:1413–1433.

30. Lutolf M, et al. Synthetic matrix metalloproteinase-sensitive hydrogels for the conduction of tissue regeneration: engineering cell-invasion characteristics. Proc Natl Acad Sci. 2003; 100:5413–5418. [PubMed: 12686696]

31. Patterson J, Hubbell JA. Enhanced proteolytic degradation of molecularly engineered PEG hydrogels in response to MMP-1 and MMP-2. Biomaterials. 2010; 31:7836–7845. [PubMed: 20667588]

32. Kim S, Healy KE. Synthesis and characterization of injectable poly (N-isopropylacrylamide-co-acrylic acid) hydrogels with proteolytically degradable cross-links. Biomacromolecules. 2003; 4:1214–1223. [PubMed: 12959586]

33. West JL, Hubbell JA. Polymeric biomaterials with degradation sites for proteases involved in cell migration. Macromolecules. 1999; 32:241–244.

34. Khetan S, Burdick JA. Patterning network structure to spatially control cellular remodeling and stem cell fate within 3-dimensional hydrogels. Biomaterials. 2010; 31:8228–8234. [PubMed: 20674004]

35. Purcell BP, et al. Injectable and bioresponsive hydrogels for on-demand matrix metalloproteinase inhibition. Nat Mater. 2014; 13:653–661. [PubMed: 24681647]

36. Burdick JA, Prestwich GD. Hyaluronic acid hydrogels for biomedical applications. Adv Mater. 2011; 23:H41–H56. [PubMed: 21394792]

37. Sundararaghavan HG, Metter RB, Burdick JA. Electrospun fibrous scaffolds with multiscale and photopatterned porosity. Macromol Biosci. 2010; 10:265–270. [PubMed: 20014198]

38. Pounder RJ, Stanford MJ, Brooks P, Richards SP, Dove AP. Metal free thiol–maleimide 'Click'reaction as a mild functionalisation strategy for degradable polymers. Chem Commun. 2008:5158–5160.

39. Lauer-Fields JL, Tuzinski KA, Shimokawa K-i, Nagase H, Fields GB. Hydrolysis of triple-helical collagen peptide models by matrix metalloproteinases. J Biol Chem. 2000; 275:13282–13290. [PubMed: 10788434]

40. Miller JS, et al. Bioactive hydrogels made from step-growth derived PEG–peptide macromers. Biomaterials. 2010; 31:3736–3743. [PubMed: 20138664]

41. Holloway JL, Ma H, Rai R, Burdick JA. Modulating Hydrogel Crosslink Density and Degradation to Control Bone Morphogenetic Protein Delivery and *In Vivo* Bone Formation. J Control Release. 2014; 191:63–70. [PubMed: 24905414]

42. Wilson EM, et al. Region-and type-specific induction of matrix metalloproteinases in post–myocardial infarction remodeling. Circulation. 2003; 107:2857–2863. [PubMed: 12771000]

43. Mukherjee, Rupak, et al. Myocardial infarct expansion and matrix metalloproteinase inhibition. Circulation. 2003; 107:618–625. [PubMed: 12566376]

44. Groblewska, Magdalena, et al. Serum levels and tissue expression of matrix metalloproteinase 2 (MMP-2) and tissue inhibitor of metalloproteinases 2 (TIMP-2) in colorectal cancer patients. Tumor Biology. 2014; 35:3793–3802. [PubMed: 24395652]

45. Incorvaia, Lorena, et al. MMP-2, MMP-9 and activin A blood levels in patients with breast cancer or prostate cancer metastatic to the bone. Anticancer Res. 2007; 27:1519–1525. [PubMed: 17595770]

46. Ji Y, et al. Electrospun three-dimensional hyaluronic acid nanofibrous scaffolds. Biomaterials. 2006; 27:3782–3792. [PubMed: 16556462]

47. Martens P, Metters AT, Anseth KS, Bowman CN. A generalized bulk-degradation model for hydrogel networks formed from multivinyl cross-linking molecules. J Phys Chem B. 2001; 105:5131–5138.

48. Tambralli A, et al. A hybrid biomimetic scaffold composed of electrospun polycaprolactone nanofibers and self-assembled peptide amphiphile nanofibers. Biofabrication. 2009; 1:025001. [PubMed: 20811101]

49. Kim HS, Yoo HS. MMPs-responsive release of DNA from electrospun nanofibrous matrix for local gene therapy: in vitro and in vivo evaluation. J Control Release. 2010; 145:264–271. [PubMed: 20347898]

50. van Dijk M, van Nostrum CF, Hennink WE, Rijkers DT, Liskamp RM. Synthesis and characterization of enzymatically biodegradable PEG and peptide-based hydrogels prepared by click chemistry. Biomacromolecules. 2010; 11:1608–1614. [PubMed: 20496905]

51. Jun HW, Yuwono V, Paramonov SE, Hartgerink JD. Enzyme-Mediated Degradation of Peptide-Amphiphile Nanofiber Networks. Adv Mater. 2005; 17:2612–2617.

52. Galler KM, Aulisa L, Regan KR, D'Souza RN, Hartgerink JD. Self-assembling multidomain peptide hydrogels: designed susceptibility to enzymatic cleavage allows enhanced cell migration and spreading. J Am Chem Soc. 2010; 132:3217–3223. [PubMed: 20158218]

53. Marklein RA, Burdick JA. Spatially controlled hydrogel mechanics to modulate stem cell interactions. Soft Matter. 2010; 6:136–143.

54. Ghasemi-Mobarakeh L, Semnani D, Morshed M. A novel method for porosity measurement of various surface layers of nanofibers mat using image analysis for tissue engineering applications. J Appl Polym Sci. 2007; 106:2536–2542.

55. Burdick JA, Chung C, Jia X, Randolph MA, Langer R. Controlled degradation and mechanical behavior of photopolymerized hyaluronic acid networks. Biomacromolecules. 2005; 6:386–391. [PubMed: 15638543]
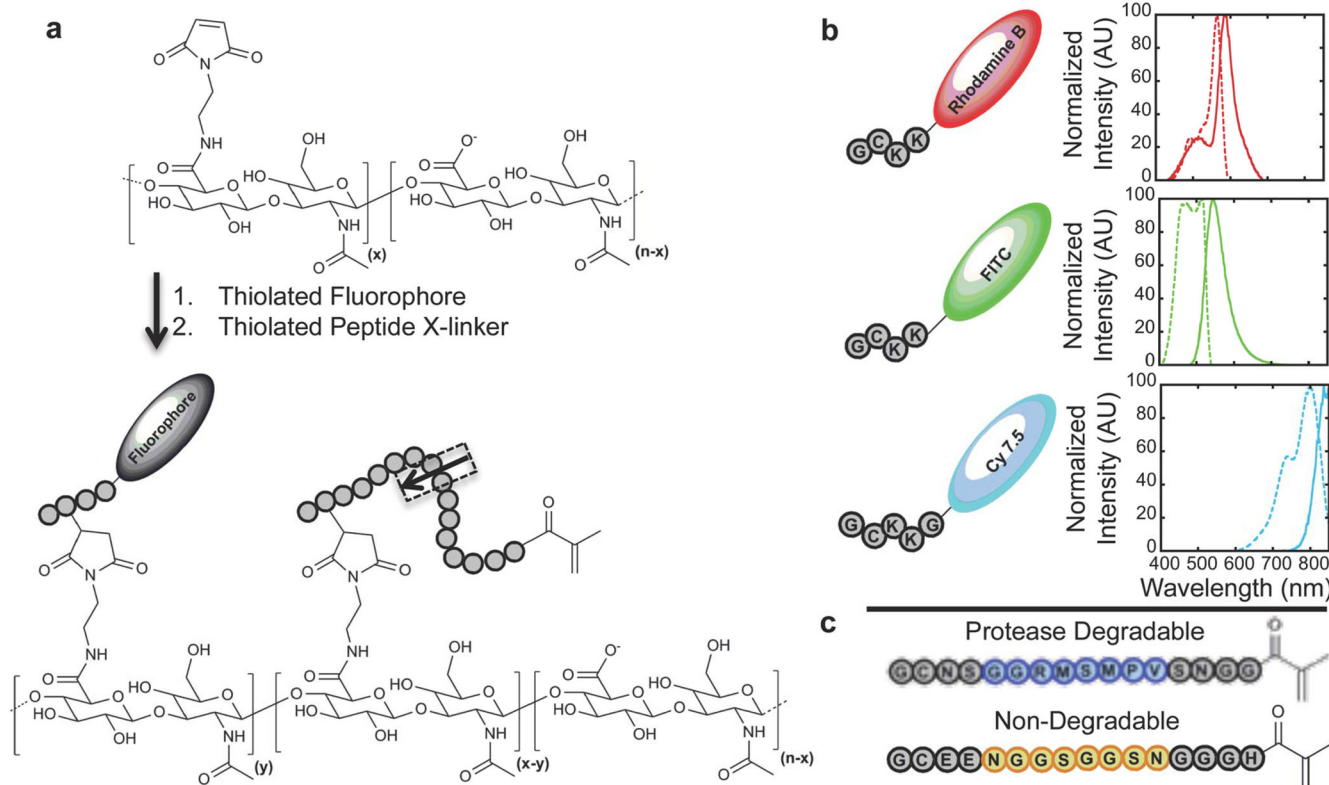
Figure 1. Synthesis and molecular design of macromer components
(**a**) Schematic of modular MePHA synthesis from the combination of maleimide HA (MaHA - top) and thiolated peptides (fluorophores or crosslinkers). Protease degradable MePHA (bottom) contains a protease mediated cleavage site (dotted rectangle) to facilitate degradation while the fluorophore facilitates monitoring of degradation and *in situ* imaging. (**b**) Thiolated peptide-fluorophores (amino acids sequences listed in circles) synthesized via solid-phase synthesis to covalently label MePHA and their corresponding excitation (dotted lines) and emission (solid lines) spectra. (**c**) Thiolated peptide crosslinkers designed to contain a thiol at one end (cysteine), a central sequence sensitive to protease degradation (blue) or insensitive to protease degradation (orange), and a photopolymerizable end group (methacrylate) to permit UV-initiated polymerization.
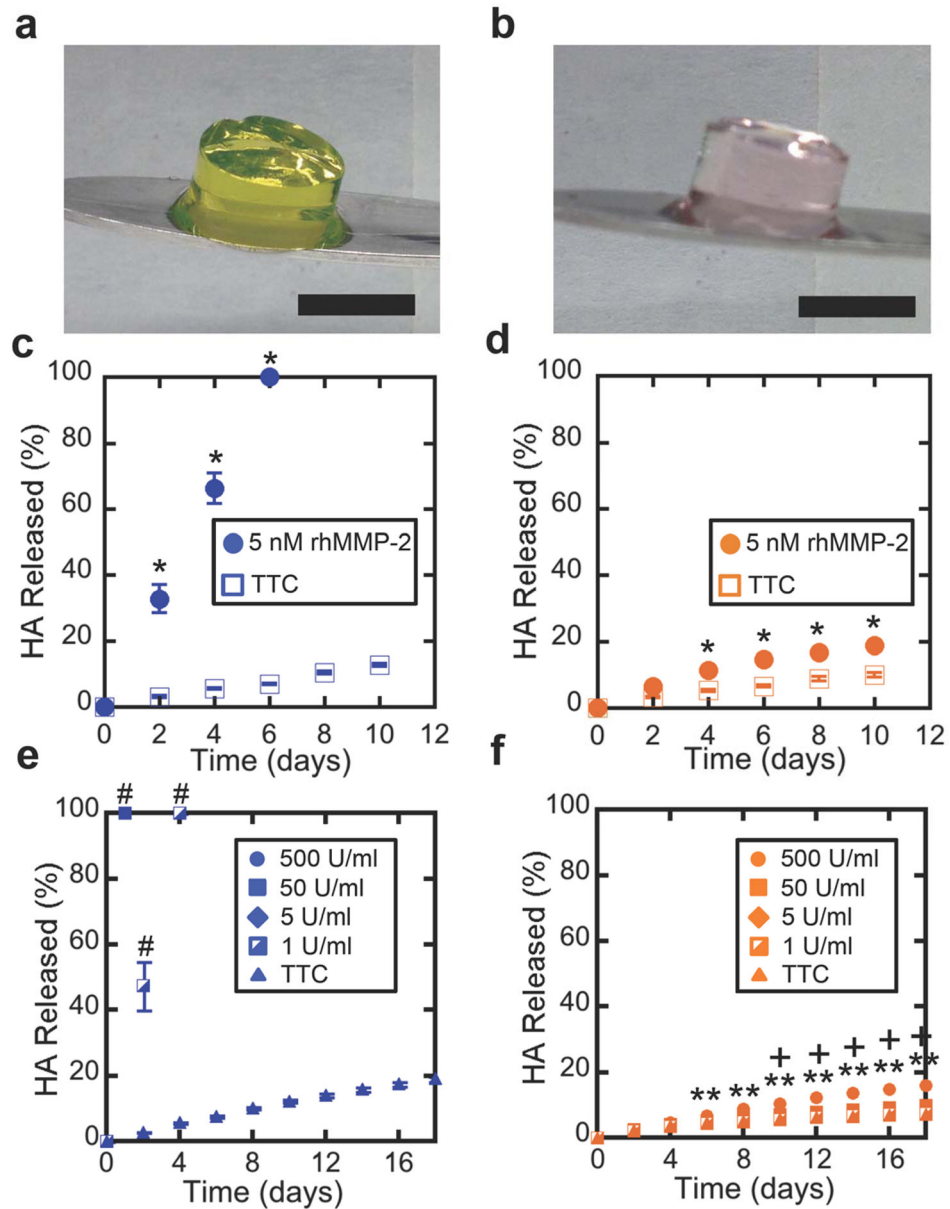
Figure 2. *In vitro* **isotropic MePHA hydrogel degradation**
50 μl non-fibrous hydrogels of protease degradable (**a**) and non-degradable (**b**) MePHA
equilibrated for 48 hours at 37°C retain their cylindrical shape. Scale bar: 5 mm. (**c,d,e,f**)
Quantification of HA release from 2 wt% MePHA hydrogels crosslinked with protease
degradable (**c,e**) or non-degradable (**d,f**) methacrylated peptides in 5nM rhMMP-2 (**c,d**),
varying concentrations of Type II collagenase (**e,f**-listed in units of activity per ml) or TTC
buffer. Media (rhMMP-2, collagenase, or TTC buffer) was refreshed every two days to
maintain enzyme activity and HA release was quantified by monitoring release of a
fluorophore covalently bonded to HA. Error bars represent S.D. (n=3,4). *p<0.05 versus
TTC. #-All isotropic protease degradable hydrogels degraded in Type II collagenase were

statistically different from control (TTC) at all time points, $p<0.05$. **$p<0.05$ 500 U ml^{-1} versus TTC, +$p<0.05$ 50 U ml^{-1} versus TTC.
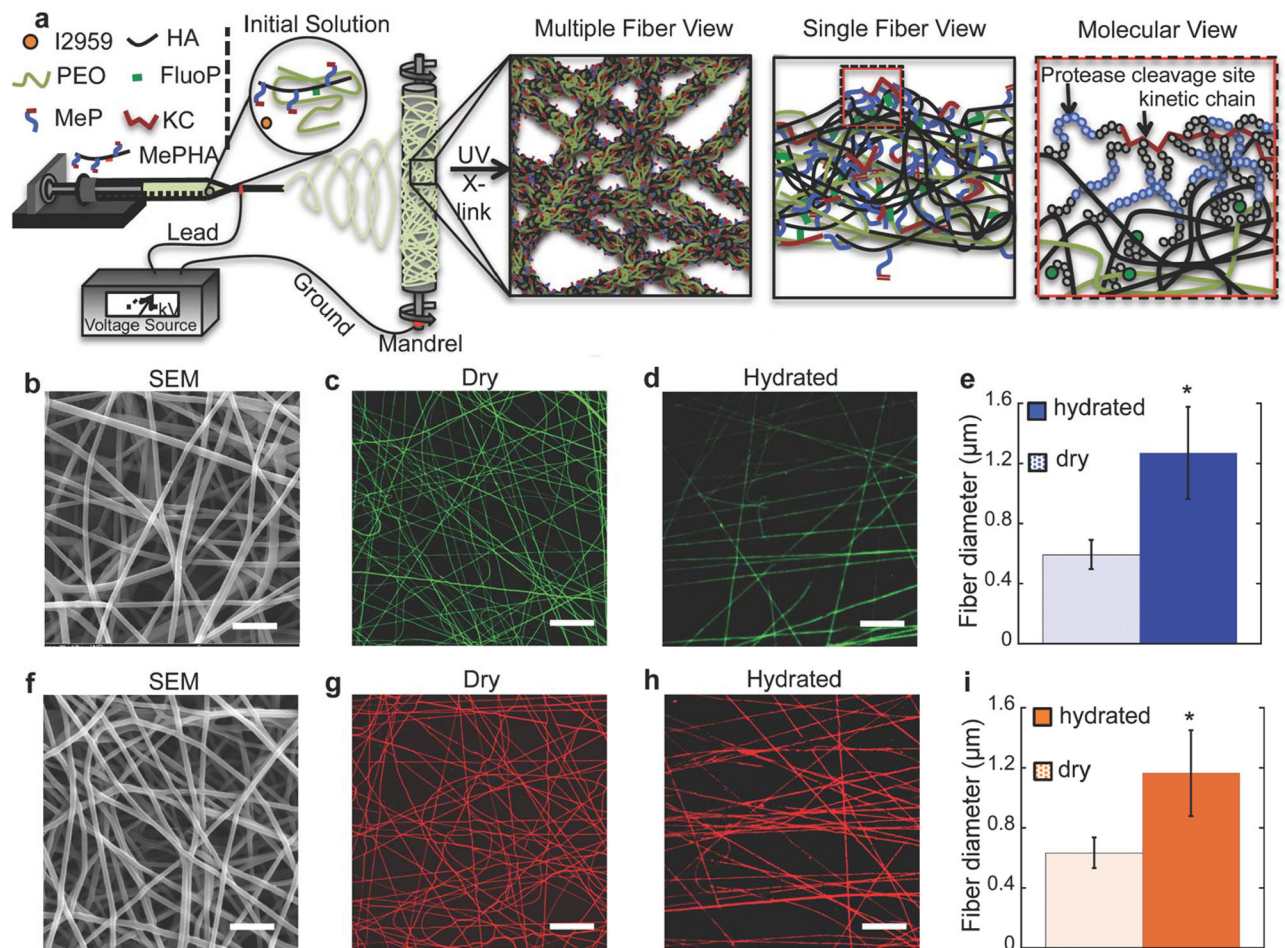
Figure 3. Electrospun fibrous MePHA hydrogel characterization
(a) Schematic of electrospinning and molecular composition of MePHA fibrous scaffolds. Molecular view highlights the sites of protease cleavage and kinetic chain formation between methacrylated peptides after crosslinking. Abbreviations: I2959 – Irgacure 2959 (photoinitiator), PEO – polyethylene oxide, MeP – methacrylated peptide, HA – hyaluronic acid, FluoP – fluorescent peptide, KC – kinetic chain, MePHA – methacrylated peptide HA. Representative SEM images of protease degradable (**b**) and non-degradable (**f**) electrospun MePHA. Fluorescent confocal microscopy images of protease degradable (**c,d**) and non-degradable (**g,h**) electrospun MePHA scaffolds in the dry and hydrated states. (**e,i**) Quantification of fiber diameters before (dry) and after swelling (hydrated) from confocal images of protease degradable (**e**) and non-degradable (**i**) MePHA scaffolds. Error bars represent S.D. *p<0.05. Scale bars: **b,f** – 2 μm, **c,d,g,h** – 25 μm.
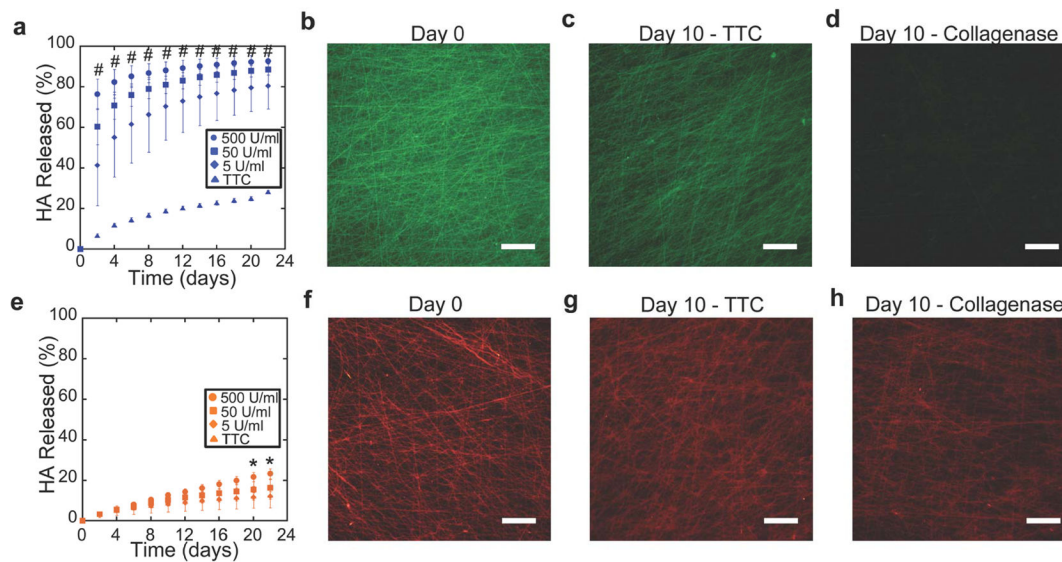
Figure 4. *In vitro* fibrous MePHA hydrogel degradation

HA release profiles of electrospun protease degradable (**a**) or non-degradable (**e**) MePHA scaffolds in varying concentrations of Type II collagenase (listed in units of activity per ml) or TTC buffer. HA release was quantified by monitoring release of a fluorophore covalently bonded to HA. Error bars represent S.D. #-All protease degradable scaffolds in Type II collagenase (500-5 U ml^{-1}) were statistically different from control (TTC) at all time points (2–22 days), p<0.05. *p<0.05 500 U ml^{-1} versus TTC. (**b–d**, **f–h**) Representative wide-field fluorescent microscopy images of thin film electrospun protease degradable (**b–d**) or non-degradable (**f–h**) MePHA scaffolds at day 0 (**b,f**) and after incubation at 37°C in TTC buffer (**c,g**) or 500 U ml^{-1} Type II collagenase (**d,h**) for 10 days. Media (collagenase or TTC buffer) was refreshed every two days for all scaffolds to maintain enzyme activity. Scale bars: 100 μm.
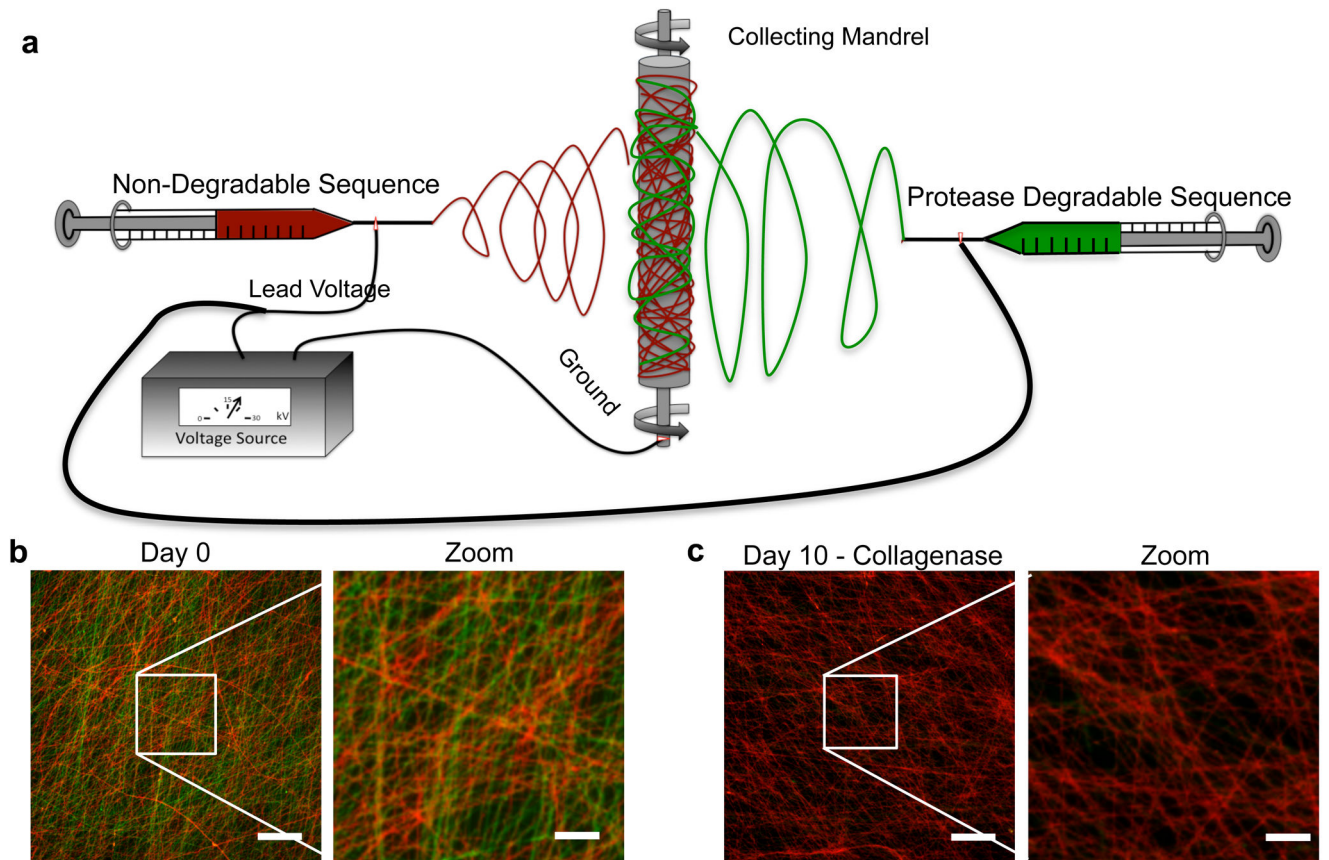
Figure 5. Co-electrospun fibrous MePHA hydrogel scaffolds
(**a**) Schematic of co-electrospinning setup to form fibrous scaffolds that contain both protease degradable (green) and non-degradable (red) MePHA fibers. (**b,c**) Representative wide-field fluorescent microscopy images of co-electrospun MePHA at day 0 (**b**) and after 10 days incubation at 37°C in 500 U ml^{-1} Type II collagenase (**c**). Media (collagenase or TTC buffer) was refreshed every two days to maintain enzyme activity. Scale bars: 100 μm, Zoom – 25 μm.
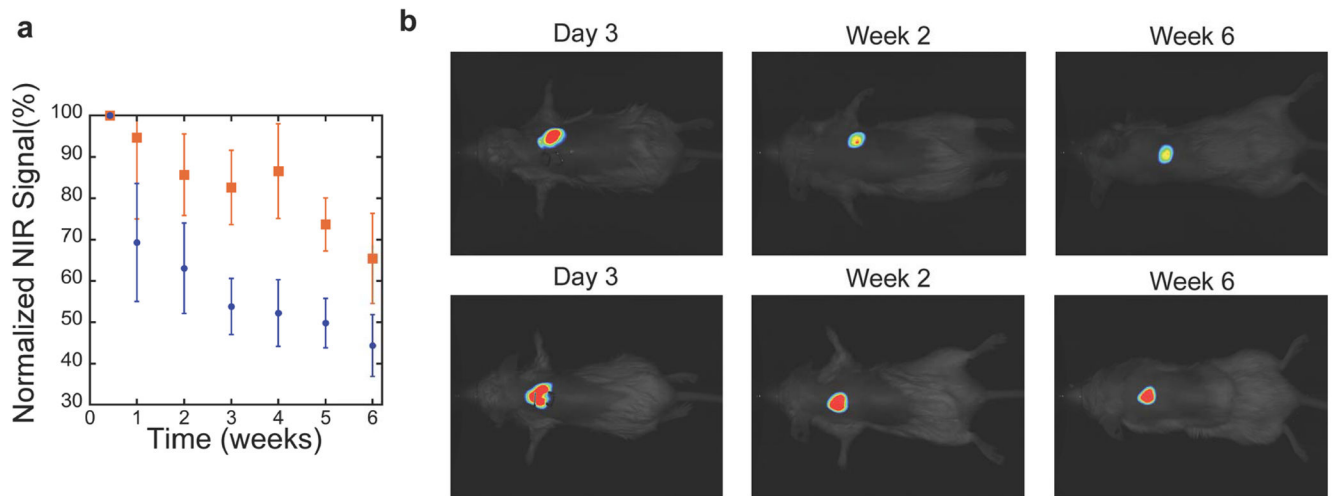
Figure 6. *In vivo* fibrous MePHA hydrogel degradation
(**a**) Erosion of protease degradable (blue) and non-degradable (orange) electrospun fibrous MePHA in a subcutaneous mouse model quantified by signal decay of a Cyanine7.5 dye covalently bonded to HA before scaffold formation. Error bars represent S.E. (n=4,3). (**b**) Representative serial *in vivo* optical images used to quantify HA release from the site of implantation.

Table 1

Kinetic parameters for peptide crosslinkers.

Peptide	Enzyme	k_{cat} s^{-1}	k_m μM	k_{cat}/k_m s^{-1} M^{-1}
Protease Degradable	rhMMP-2	3.2 ± 0.9	2100 ± 900	1800 ± 900
Protease Degradable	Type II collagenase	0.65 ± 0.07	3090 ± 450	210 ± 35
Non-Degradable	rhMMP-2	N.M.	N.M.	N.M.
Non-Degradable	Type II collagenase	N.M.	N.M.	N.M.

N.M.= not measurable. Non-degradable peptides showed no detectable degradation during incubation in rhMMP-2 or Type II collagenase. Error listed as standard deviation of three separate non-linear regression fits.